Kinetic Scheme for Thymidylate Synthase from *Escherichia coli*: Determination from Measurements of Ligand Binding, Primary and Secondary Isotope Effects, and Pre-Steady-State Catalysis†

H. Trent Spencer,*,‡ J. Ernest Villafranca,§ and James R. Appleman‡,||

Department of Molecular Pharmacology, St. Jude Children's Research Hospital, Memphis, Tennessee 38101, and Agouron Pharmaceuticals, Inc., 3565 Atomics Court, San Diego, California 92121

Received July 22, 1996; Revised Manuscript Received December 11, 1996⊗

ABSTRACT: We have determined kinetic and thermodynamic constants governing binding of substrates and products to thymidylate synthase from *Escherichia coli* (TS) sufficient to describe the kinetic scheme for this enzyme. (1) The catalytic mechanism is ordered in the following manner, TS + dUMP → TS·dUMP + (6*R*)-5,10-CH_2-H_4folate → TS·dUMP·(6*R*)-5,10-CH_2H_4folate → TS·dTMP·H_2folate → TS·dTMP → TS as predicted previously by others from steady-state measurements. (2)When substrates are saturating, the overall reaction rate is governed by the slow conversion of enzyme-bound substrates to bound products as demonstrated by (i) large primary and secondary isotope effects on k_{cat} and (ii) high rates of product dissociation compared to k_{cat}. (3) Stopped-flow studies measuring the binding of 10-propargyl-5,8-dideazafolate, an analog of (6*R*)-5,10-CH_2H_4folate, with the active site mutant C146A or the C-terminus-truncated mutant P261Am enabled us to identify physical events corresponding to spectral changes which are observed with the wild-type enzyme during initiation of catalysis. A kinetically identifiable reaction step, TS·dUMP·(6*R*)-5,10-CH_2H_4folate → (TS·dUMP·(6*R*)-5,10-CH_2H_4folate)*, likely represents reorientation of the C-terminus of the enzyme over the catalytic site. This seals the substrates into a relatively nonaqueous environment in which catalysis can occur. (4) Although TS is a dimer of identical subunits, catalysis is probably confined to only one subunit at a time. (5) The "high-resolution" kinetic scheme described herein provides a framework for the interpretation of the kinetics of catalysis by mutant ecTS chosen to provide insights into the relationship between structure and function.

Thymidylate synthase (TS)[1] (methylenetetrahydrofolate: dUMP C-methyltransferase, EC 2.1.1.b) catalyzes the conversion of dUMP and (6*R*)-5,10-CH_2H_4folate (CH_2H_4folate) to dTMP and H_2folate by reductive methylation, in which CH_2H_4folate serves as both methyl donor and reducing agent. TS plays a critical role in pyrimidine biosynthesis by providing the only *de novo* source of dTMP, which is required for DNA synthesis. Maintaining adequate levels of dTMP is particularly important in dividing cells where DNA synthesis is rapid. Because this reaction is the only known *de novo* source of dTMP, TS has been a logical target for the design of chemotherapeutic agents.

TS consists of two identical subunits with a dimeric molecular weight of approximately 60 000. Comparison of 17 known sequences for TS shows that it is among the most highly conserved enzymes (Perry et al., 1990). The high number of conserved residues is believed to be due to the importance of the reaction which TS catalyzes and possibly to the conformational dynamics occurring throughout the protein which result from substrate binding. Recombinant TS from *Escherichia coli* (ecTS) (Dev et al., 1988; Matthews et al., 1990a), *Lactobacillus casei* (lcTS) (Pinter et al., 1988; Climie & Santi, 1990) Bacteriophage T4 (Finer-Moore et al., 1994), *Pneumocystis carinii* (Edman et al., 1989), *Candida albicans* (Singer et al., 1989), murine (Zhang et al., 1989, 1990), and human (hTS) (Davisson et al., 1989) have become readily available in relatively large quantities. Investigations into the functional role of certain amino acid residues in these enzymes are underway through comparison of the steady-state catalytic properties and kinetics of inhibitor binding to wild-type enzyme with mutants generated by oligonucleotide-directed mutagenesis (Appleman et al., 1991; Climie et al., 1992; Dev et al., 1988, 1994; LaPat-Polasko et al., 1990; Maley & Maley, 1988; Michaels et al., 1990; Zhang et al., 1990; Hardy et al., 1995). Crystallographic structures for lcTS (Hardy et al., 1987; Perry et al., 1990; Finer-Moore et al., 1993), ecTS (Montfort et al., 1990; Perry et al., 1990), and hTS (Schiffer et al., 1995) complexed with a variety of substrates and inhibitors and at

† This work was supported by United States Public Health Service Research Grant R29 GM 45367 (to J.R.A.), National Research Service Award (to H.T.S.), and by the American Lebanese Syrian Associated Charities (to J.R.A. and H.T.S.).

* To whom correspondence should be addressed. Present address: Department of Chemistry and Biochemistry, University of South Carolina, 730 S. Main Street, Columbia, SC 29208. E-mail: Spencer@psc.psc.sc.edu.

‡ St. Jude Children's Research Hospital.

§ Agouron Pharmaceuticals, Inc.

|| Present address: Gensia Pharmaceuticals, Inc., San Diego, CA 92121.

⊗ Abstract published in *Advance ACS Abstracts,* April 1, 1997.

[1] Abbreviations: TS, thymidylate synthase (methylenetetrahydrofolate:dUMP C-methyltransferase, EC 2.1.1.b); ecTS, TS from *E. coli*; lcTS, TS from *L. casei*; hTS, human TS; CH_2H_4folate, (6*R*)-5,10-CH_2-H_4folate; H_3Dfolate, (6*S*)-[6-^{2}H]H_4folate; CH_2H_3Dfolate, (6*R*)-5,10-CH_2-[6-^{2}H]H_4folate; CD_2H_4folate, (6*R*)-5,10-[$^2H_2$]CH_2-H_4folate; CD_2H_3-Dfolate, (6*R*)-5,10-[$^2H_2$]CH_2-[6-^{2}H]H_4folate; FdUMP, 5-fluoro-2′-deoxyuridylate; PDDF, 10-propargyl-5,8-dideazafolate; C146A, TS mutant with the active site cysteine replaced with alanine; P261Am, TS mutant lacking the four C-terminal amino acid residues.

S0006-2960(96)01794-1 CCC: $14.00

high resolution provide a framework for the structural interpretation of such studies into the mechanism of catalysis and inhibition. However, a detailed kinetic scheme for wild-type enzyme has not yet been described. Therefore, interpretation of the results of experiments with certain mutant enzymes is at least in some cases ambiguous.

Crystallographic studies clearly indicate the presence of a distinct catalytic site on each subunit. Nonetheless, in the absence of folates, the nucleotides dUMP, dTMP, and FdUMP bind to a single site on TS from many sources [for example, see Galivan et al. (1976) and Dev et al. (1988)]. At least for lcTS, an equilibrium exists between non-covalent and covalent binding involving an invariant cysteine on the enzyme (Cys146 for ecTS) and the 5 position of the nucleotide, with the non-covalent complex favored (Moore et al., 1986a). Upon binding of reduced folates such as H_2-folate, H_4folate, and CH_2H_4folate, the equilibrium is altered so that, with dUMP and FdUMP, most nucleotide is covalently linked to the enzyme (Moore et al., 1986b). Furthermore, for at least some complexes a second site for nucleotide and folate binding becomes accessible, although affinity at this second site is substantially lower than at the first site (Galivan et al., 1976; Dev et al., 1994).

In the absence of nucleotides, binding of folates is sufficiently weak that it cannot be detected (Galivan et al., 1976). This is not surprising since bound nucleotide forms an integral part of the folate binding site [for example, see Matthews et al. (1990a,b)]. However, the normal intracellular form of folates are polyglutamates, which bind substantially tighter to both free and enzyme−nucleotide complexes. For example, the dissociation constant for pteroyltetraglutamate with lcTS was found to be 36 μM by equilibrium dialysis whereas no evidence of binding by pteroylmonoglutamate was found, even at a concentration of 500 μM (Galivan et al., 1977).

The simultaneous occupancy of the folate and nucleotide site triggers a transition between free TS (open form) and bound TS (closed form). After ligand binding, conformational changes occur that sequester both ligands from the solvent. Most notable changes are observed at the C-terminus (Finer-Moore et al., 1993; Kamb et al., 1992; Matthews et al., 1990a; Montfort et al., 1990). In the absence of ligand, the C-terminus, approximately four residues, shows very little constraint. Upon the binding of CH_2H_4folate the C-terminus folds over the folate binding site and forms a hydrogen bonding network with several atoms of the bound cofactor. Disrupting the hydrogen bonding network by treatment with carboxypeptidase A (CPA) or directed mutagenesis results in a protein that is catalytically inactive (Aull et al., 1974; Galivan et al., 1976; Cisneros et al., 1993; Carreras et al., 1992; Climie et al., 1992). These results indicate that the dramatic conformational changes occurring at the C-terminus, leading to the closed form of the molecule, are required for catalytic activity. The truncated enzymes, however, are still able to covalently bind FdUMP and form a ternary complex between FdUMP and CH_2H_4folate and to carry out other partial reactions like dehalogenation of 5-bromo- and 5-iodo-dUMP.

Although an active site is present on both subunits, there is debate as to whether the active sites function independently, if catalytic activity alternates between subunits, and to what degree of coordination exists between subunits (Hardy et al., 1987; Montfort et al., 1990; Matthews et al., 1990a,b; Bradshaw & Dunlap, 1993; Dev et al., 1994; Reilly et al, 1995). It is believed that substrate binding and product release are ordered with dUMP binding first, initially to a single subunit, followed by CH_2H_4folate binding to the same subunit occupied by dUMP [reviewed in Santi and Danenberg (1984)]. The rapid conversion of dUMP to dTMP when CH_2H_4folate is present has so far prevented characterization of the number of nucleotide binding sites in this ternary complex (i.e., TS with dUMP and CH_2H_4folate). Dev et al. (1994) showed by measuring the binding of folate and folate analogs that the two catalytic sites exhibit induced negative cooperativity and that the asymmetric binding of ligands is the predominant factor that determined inhibition kinetics. Asymmetry of nucleotide binding was shown by Reilly et al. (1995) for the interaction of FdUMP with human TS. The K_d for FdUMP binding to the first site was much lower than at the second due to differences in k_{on} between the two sites. Heterodimeric TS mutants have been constructed and should provide insights into the mechanism of cooperativity employed by this enzyme [reviewed in Carreras and Santi (1995)]. Nonetheless, the issue of the number of active sites per dimer remains unresolved even though a variety of mutants with only a single active site per dimer are available.

Scheme 1: Order of Substrate Binding and Product Release during the Catalytic Cycle of TS on the Basis of Initial Velocity and Product Inhibition Studies [Reviewed by Carreras and Santi (1995)][a]

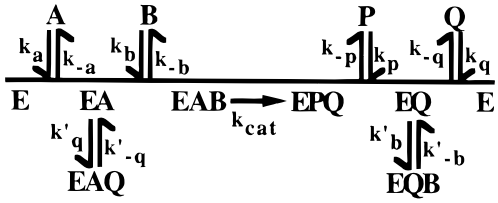

[a] Under certain conditions, this order may be altered with methylenefolylpolyglutamate as substrates. The species are E, ecTS; A, dUMP; B, CH_2H_4folate; P, H_2folate; Q, dTMP. The second-order rate constants k_{-a}, k_{-b}, k_{-p}, and k_{-q} are dissociation rate constants, and k_{cat} is an apparent first-order rate constant describing the rate of net conversion of enzyme-bound substrates to bound products. The rate constants k'_q, k'_{-q}, k'_b, and k'_{-b} describe formation and breakdown of abortive complexes.

The individual reaction steps involved in catalysis by TS may be divided into two categories: those involved in binding and dissociation of substrates and products (Scheme 1) and the series of chemical reactions in which enzyme-bound substrates are converted to bound products (Scheme 2). To further elucidate and refine the kinetic scheme we have generated mutant enzymes by oligonucleotide-directed mutagenesis. C146A has the active site cysteine replaced with alanine which prevents covalent attack by TS on dUMP, resulting in a catalytically inactive enzyme. However, processes preceding nucleotide attack by Cys146, e.g., ligand binding and C-terminus closure over the substrate binding pocket, are not affected. P261Am lacks the four C-terminal amino acid residues making it impossible for the C-terminus to close over the substrate binding site. The analog PDDF was utilized because it undergoes reactions similar to the first few catalytic steps. Interpretation of the kinetics with this ligand and the crippled mutants is much simpler than with the wild-type enzyme and the natural substrates because the reactions do not proceed past ternary complex formation. In this study, directly measured values of rate and equilibrium constants for individual steps depicted in these schemes are reported and are sufficient to define an operational kinetic scheme for catalysis by ecTS. This scheme provides a

Scheme 2: Chemical Reactions Involved in Catalysis[a]

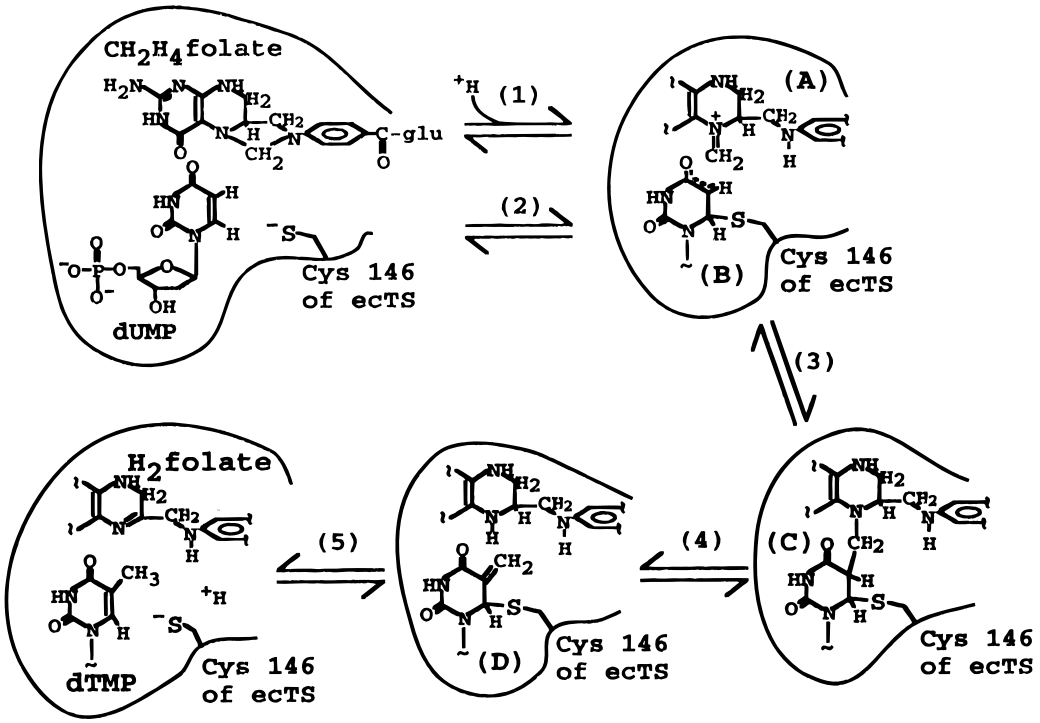

[a] Upon binding dUMP to TS, an equilibrium is established between non-covalent TS·dUMP and covalent TS−dUMP complexes (reaction 2). Binding of CH_2H_4folate shifts the equilibrium in favor of TS−dUMP (B). It is believed that the binding site for the folate is constructed so that it facilitates formation of the N5-iminium ion CH_2^+═H_4folate (A), which is subsequently attacked by the dUMP enolate ion to form a covalent ternary complex (C). Such a covalent ternary complex has been isolated by trichloroacetic acid precipitation of enzyme within a few seconds after mixing with both substrates (Moore et al., 1986b). Stereochemical considerations indicate that this intermediate must undergo a conformational isomerization before eliminating H_4folate and a proton, generating an exocyclic methylene on the enzyme-bound nucleotide (D). The methylene is reduced by H_4folate, and the 5,6 double bond is regenerated by elimination to form dTMP and enzyme.

framework for the interpretation of current studies into the kinetics of catalysis by mutant ecTS generated by oligonucleotide-directed mutagenesis that are designed to yield insights into the relationship between structure and function.

EXPERIMENTAL PROCEDURES

Materials. dUMP, dTMP, FdUMP, folate, $NADP^+$, and NADPH were from Sigma. Formaldehyde and $MgCl_2$ were from Fischer. [$^2H_2$]Formaldehyde was from Cambridge Isotope Laboratories. (4*R*)-[^{2}H]NADPH (NADPD), (6*S*)-H_4folate, and ecTS were prepared essentially as described previously (Beard et al., 1989; Appleman et al., 1990; Dev et al., 1988). (6*R*)-5,10-CH_2-H_4folate (CH_2H_4folate) was prepared from H_4folate by incubation with formaldehyde. (6*S*)-6-[^{2}H]H_4folate (H_3Dfolate) was prepared by the stereospecific reduction of H_2folate with NADPD using recombinant human dihydrofolate reductase and converted to (6*R*)-5,10-CH_2-[6-^{2}H]H_4folate (CH_2H_3Dfolate) by incubation with formaldehyde. (6*R*)-5,10-[$^2H_2$]CH_2H_4folate (CD_2H_4-folate) and (6*R*)-5,10-[$^2H_2$]CH_2-[6-^{2}H]H_4folate (CD_2H_3-Dfolate) were prepared by incubation of H_4folate and H_3Dfolate, respectively, with [$^2H_2$]formaldehyde.

Production and Purification of Wild-Type and Mutant Enzymes. Wild-type *Escherichia coli* thymidylate synthase (ecTS) was isolated from *E. coli* transformed with a high-amplifying expression plasmid containing the ecTS gene and *E. coli* fol promoter as previously described (Villafranca *et al.*, 1983). The ecTS gene was mutated by the method of Kunkel (1985) using the Bio-Rad Mut-A-Gene M13 *in vitro* Mutagenesis Kit. Purification of U-containing ssM13MP18 containing the TS gene or mutated gene, phosphorylation of the oligonucleotides, annealing of the oligonucleotides with the template, polymerase extension of the mutagenic strand, and transformation into MV1190 cells were carried out according to the recommendations of the manufacturer. Single-stranded phage DNA was screened for successful mutagenesis by sequencing over the target site. For the production of plasmid DNA, positive mutants were infected into JM103 cells. The mutated fragment (*Bam*H1 to *Hin*dIII) was cloned into pUC8 which was used to transform *E. coli* Rue 10 cells. Ampicillin resistant colonies were cultured in YT media. Wild-type TS and mutant enzymes were isolated from the transformed *E. coli* by FPLC on Q-Sepharose (55 mL column, eluted with a 150−400 mM KCl gradient in 50 mM Tris, 20 mM 2-mercaptoethanol, 1 mM EDTA, pH 7.4) and phenyl Sepharose [30 mL column, eluted with an initial gradient of 1 M $(NH_4)_2SO_4$ to 0.7 M $(NH_4)_2$-SO_4 to 0 M $(NH_4)_2SO_4$, in 50 mM Tris, 20 mM 2-mercaptoethanol, 1 mM EDTA]. Residual dihydrofolate reductase activity was removed by methotrexate affinity chromatography using gradients of 0−100 mM KCl, 100−350 mM KCl, and 350−1000 mM KCl all in Tris, 2-mercaptoethanol, EDTA buffer. Purified protein was frozen in liquid nitrogen and stored at −80 °C. Enzyme purity was indicated by a single band on SDS−PAGE and non-denaturing PAGE. The absence of catalytic activity, i.e., product formation, with 5 μM C146A or 5 μM P261Am in the presence of 100 μM dUMP and 100 μM CH_2H_4folate indicates the mutant enzyme preparations were not significantly contaminated with wild-type enzyme. Before use each enzyme was applied to a PD-10 column (Pharmacia) equilibrated in activation buffer composed of 100 mM Tris, 50 mM 2-mercaptoethanol, and 0.1 mM EDTA.

Enzyme Concentration. Although the value of the molar extinction coefficient ϵ has yet to be reported for ecTS, a reasonably accurate value can be calculated from the amino acid composition. Since ecTS contains 18 tyr and 14 trp, ϵ_{280} is expected to be 1.02×10^5 M^{-1} cm^{-1} at pH 13. From this value and from the measured ratio of A_{280} for ecTS at pH 7.4 and 13, ϵ_{280} at pH 7.4 is calculated to be 1.13×10^5 M^{-1} cm^{-1}. The latter value, which is similar to that of lcTS (1.07×10^5 M^{-1} cm^{-1} at pH 6.8; Santi et al., 1974) containing 22 tyr and 12 trp, has been utilized to determine ecTS concentration. All reported concentrations refer to dimeric enzyme rather than to the number of ligand binding sites unless otherwise noted. The enzyme has 1.9 ± 0.1 binding sites per molecule ecTS for the inhibitor 5-fluoro-2′-deoxyuridylate (FdUMP) in the presence of CH_2H_4folate.

Experimental Conditions and Enzyme Assays. Measurements were made in a buffer mixture containing 100 mM Tris, 50 mM 2-mercaptoethanol, 1 mM EDTA, pH 7.4, and at 20 °C except where noted. ecTS was assayed by monitoring the increase in absorbance at 340 nm accompanying conversion of CH_2H_4folate to H_2folate ($\Delta\epsilon_{rxn} = 6.4$ mM^{-1} cm^{-1}). The standard deviation for the reported steady-state parameters is less than 10% unless noted otherwise.

Equilibrium Dissociation Constants. Dissociation constants for the interaction of ligands with enzymes were determined by titrating the change in enzyme fluorescence that accompanies complex formation as described previously (Appleman et al., 1988a,b, 1990) Corrections for ligand fluorescence, when present, and inner filter effects were calculated from parallel titrations in which enzyme was absent or replaced, respectively, with a quantity of tryptophan with a fluorescence intensity equal to that of the enzyme. A more complete description for the evaluation of ligand binding is presented in the Appendix.

Stopped-Flow Spectroscopy. The progress of ligand interactions with ecTS, C146A, or P261Am was followed by stopped-flow fluorescence or absorbance spectroscopy on a Hi Tech Scientific PQ-SF 53 spectrophotometer or Applied Photophysics at 20 °C in activation buffer. An excitation wavelength of 295 nm and emission wavelengths greater than 330 nm were used for fluorescence measurements. Enzymes and ligands were diluted in activation buffer to concentrations two times that indicated within the text or in figure legends. For experiments requiring preincubation of enzymes with dUMP, incubation was on ice for at least 5 min. After collection, data were transferred to a Macintosh Quadra 950 and computer fitted using the program Kaleidograph by nonlinear least-squares analysis to equations describing single or multiple exponential terms (see text for appropriate equations). Values of χ^2 and variance of the experimental data to the fitted data were utilized to determine best-fit curves. Each experiment was repeated at least three times. The standard deviation is less than 15% of the mean unless otherwise noted. With the exception of titration experiments pseudo-first-order binding conditions were employed.

RESULTS AND DISCUSSION

General Strategy. In this study we have directly measured association and dissociation constants for formation of enzyme−ligand complexes wherever possible. Values of remaining rate constants were calculated from the time course of transients observed during pre-steady-state catalysis, from isotope effects on steady-state catalytic rates, or from consideration of thermodynamic equilibria.

Table 1: Primary and Secondary Kinetic Isotope Effects on k_{cat}

S_1	S_2	$k_{cat}(S_1)/k_{cat}(S_2)$	isotope effect
CH_2H_4folate	CH_2H_3Dfolate	3.72 ± 0.12	primary
CH_2H_4folate	CD_2H_4folate	1.40 ± 0.08	secondary
CH_2H_3Dfolate	CD_2H_3Dfolate	1.35 ± 0.08	secondary[a]

[a] In addition to the primary effect that occurs with both substrates S_1 and S_2.

Primary and Secondary Isotope Effects on k_{cat}. When CH_2H_3Dfolate is substituted for CH_2H_4folate a large primary isotope effect is observed during steady-state catalysis (Table 1). This indicates that the reductive step involving transfer of H6 of H_4folate (reaction 5, Scheme 2) is rate-limiting in the overall catalytic cycle and that dissociation of the products must be much faster than this step. One interpretation is that after binding, substrates are rapidly converted to bound H_4folate and species D which slowly react to form the final products H_2folate and dTMP. However, large normal secondary kinetic isotope effects on k_{cat} are observed when either CD_2H_4folate or CD_2H_3Dfolate are substrates (Table 1), whereas a large inverse secondary isotope effect is anticipated for reaction 5. Furthermore, the ratios of k_{cat} for CH_2H_4folate to CD_2H_4folate and CH_2H_3Dfolate to CD_2H_3Dfolate are similar (Table 1), demonstrating that the magnitude of this secondary isotope effect is independent of the primary isotope effect. It would instead be anticipated that the measured secondary isotope effect should be greatly diminished for CH_2H_3Dfolate/CD_2H_3Dfolate versus CH_2H_4folate/CD_2H_4folate if both primary and secondary isotope effects are simple kinetic effects. The simplest interpretation of these results is that one or more steps prior to reaction 5 are in rapid equilibrium with one another and that product formation for these intervening reaction steps are thermodynamically unfavorable. The overall reaction is driven forward by reaction 5, which in the forward direction (H_2folate and dTMP formation) must be extremely energetically favorable since the overall reaction is effectively irreversible (Carreras & Santi, 1995; Hardy et al., 1995).

The question arises as to which of the folate intermediates in Scheme 2 (A, C, or H_4folate) are at highest concentration during catalytic cycling. Although we have no direct proof at this point, the following lines of evidence indicate that the net equilibrium in reactions 1, 3, and 4 probably favors enzyme-bound CH_2H_4folate versus any of the intermediates: (1) The complex with H_4folate can be eliminated because of the large normal 2° isotope effect described above, whereas an inverse effect would be observed if this complex predominated. (2) When FdUMP is substituted for dUMP, formation of the species corresponding to C is accompanied by an increase in absorbance in the near UV (readily observable at 400 nm) that is not observed in the transient-state catalysis with dUMP (unpublished results). This indicates that C is unlikely to accumulate to any appreciable extent during catalysis. (3) Since the bridge carbon in CH_2H_4folate retains an sp^3 hybridization state in both initial substrate and in final product (6-methyl of dTMP), the magnitude of the secondary isotope effect is surprisingly large even with dideutero substitution. This is particularly true since reaction 5 must be essentially irreversible (since the overall reaction is essentially irreversible) and will have

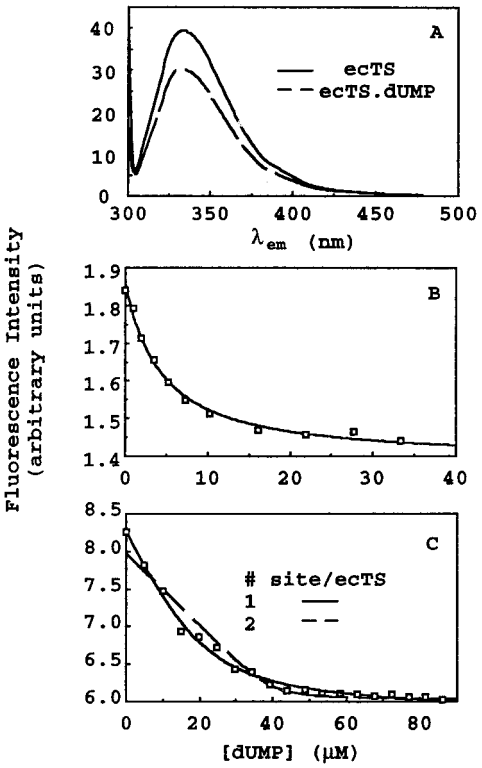

FIGURE 1: Binding of dUMP to ecTS. (A) Fluorescence emission spectra for ecTS and its complex with dUMP when excited with light of 295 nm; enzyme concentration was 1 μM. (B) Dependence of enzyme fluorescence on dUMP concentration as ecTS (1 μM) is titrated with ligand. (C) Dependence of enzyme fluorescence on dUMP concentration as ecTS (20 μM) is titrated with ligand. K_d values from analysis of these data are 4.9 ± 0.8 and 0.4 ± 0.6 μM for one- and two-site models, respectively. When the enzyme concentration is treated as the fitted parameter, $K_d = 4.2 \pm 1.4$ μM and the concentration of enzyme is 21.8 ± 3.0 μM (equivalent to 1.1 sites).

an inverse kinetic isotope effect. It seems unlikely that normal 2° isotope effects accompanying reaction 4 could overcome inverse effects for reactions 2 and 5 as would be required if A represented the preferred bound form. Thus, by elimination, we conclude that the equilibrium rapidly achieved among the bound folate intermediates must favor the unaltered substrate, CH_2H_4folate.

Kinetics and Thermodynamics of dUMP and dTMP Binding. Association of dUMP to ecTS and dissociation of dTMP from ecTS·dTMP are the first and last steps, respectively, in the catalytic cycle. Binding of dUMP to ecTS quenches the intrinsic protein fluorescence of the enzyme (Figure 1A). Values of the dissociation constant (K_d) for dUMP binding can be determined from the dependence of fluorescence intensity upon nucleotide concentration (Figure 1B, Table 2). When the enzyme concentration is much greater than K_d, this dependence is also a function of the concentration of nucleotide binding sites on the enzyme. One versus two-site models for binding of dUMP to ecTS at high enzyme concentrations are compared in Figure 1C. Analysis of this data indicates that only one dUMP binding site per dimeric TS is available in the absence of folates as demonstrated by the much better fit of the one-site versus two-site model and the good agreement in the calculated value of K_d at low and high enzyme concentrations for the one-site model (Figure 1C and Table 2) (see Appendix for mathematical treatment and further discussion). That only one binding site exists is consistent with the findings of Dev et al. (1988) with ecTS and Galivan et al. (1976) with lcTS. We have also observed similar results with lcTS (data not shown).

When ecTS or the active site mutant C146A is mixed with dUMP, the observed fluorescence intensity rapidly decreases with time as the ligand binds to enzyme (Figure 2A). The rate of binding is greater at high concentrations of dUMP than at low concentrations. For a simple bimolecular association reaction opposed by a unimolecular dissociation reaction as depicted for dUMP binding to ecTS in Scheme 1, it may be shown that under pseudo-first-order conditions ([ecTS] $\ll K_d$) the time course of fluorescence decrease at each concentration of dUMP has the form: $F_t = (\Delta F)e^{-k_{obs}t} + F_{equ}$, where F_t is fluorescence at time t, ΔF is the amplitude of the fluorescence decrease, k_{obs} is an apparent first-order rate constant, and F_{equ} is the fluorescence at equilibrium. If Scheme 1 is an adequate description of dUMP binding to ecTS, then $k_{obs} = k_a$[dUMP] $+ k_{-a}$, where k_a and k_{-a} are association (k_{on}) and dissociation (k_{off}) rate constants governing dUMP binding, respectively. Such linear dependence of k_{obs} on dUMP is indeed observed (Figure 2B), and values of k_{on} and k_{off} calculated from this dependence are reported in Table 2. Furthermore the ratio of k_{off}/k_{on} should be equal to the thermodynamically measured value of K_d, and excellent agreement is obtained. Results obtained with C146A are similar to those observed with the wild-type enzyme (Table 2), indicating that this mutation does not substantially alter the affinity for dUMP, which is in agreement with results of Dev et al. (1988).

In general, the results with dTMP are similar to those with dUMP. However, dTMP binds 3.8-fold weaker compared to dUMP. The weaker binding is a consequence of both a decrease in the rate of association (6.2 μM^{-1} s^{-1}; 1.6-fold smaller k_{on}) and faster rate of dissociation (83 s^{-1}; 2.0-fold larger k_{off}).

The results concerning the kinetics of nucleotide binding are in marked contrast to those of Middlestadt and Schmerlik (1986) with lcTS where the dependence of k_{obs} on nucleotide concentration was reported to be hyperbolic. These authors attributed this behavior to the rapid formation of an lcTS·dUMP complex in which dUMP was very weakly bound followed by a second reaction step, probably formation of the covalent link between enzyme and nucleotide, which produced a large increase in binding affinity. However, the equilibrium between non-covalent lcTS·dUMP and covalent lcTS−dUMP complexes is greatly in favor of the non-covalent form (Moore et al., 1986a,b), indicating that the second step cannot represent covalent complex formation. In addition to the difference in enzyme sources compared to this study, Middlestadt and Schmerlik carried out their measurements in KP_i buffer. It is known that phosphate competes for binding of nucleotide. We therefore chose to examine the kinetics of dUMP binding in phosphate buffer in order to determine whether differences in buffer composition might be the cause of the difference in kinetic behavior observed with the two enzymes. We found that the dependence of k_{obs} on dUMP concentration remained linear in a buffered solution containing 10 mM KP_i and 50 mM 2-mercaptoethanol, an identical phosphate concentration to that used in the study with lcTS. Furthermore, the value of k_{on} was decreased only 2.6-fold and k_{off} was essentially unchanged (Table 2) which is consistent with phosphate binding weakly to TS and competitively with dUMP. Also, we observed that the kinetics of dUMP binding to lcTS was

Table 2: Kinetic and Thermodynamic Constants for dUMP Binary Complex Formation[a]

enzyme	k_{on} (10^{-6} M^{-1} s^{-1})	k_{off} (s^{-1})	k_{off}/k_{on}[b] (10^{-6} M)	K_d[c] (10^{-6} M)	stoichiometry[d]
wild-type	9.8	41	4.2	3.9	1.1
wild-type (KP_i)[e]	3.8	38	10.1		1.1
C146A	14.6	53	4.1	7.8	0.9

[a] Standard deviation of all parameter values are less than 10%. For dUMP fluorimetric titrations, approximately 30% of the initial fluorescence was quenched upon dUMP binding. [b] Thermodynamic dissociation constant for the formation of the binary complex calculated from k_{on}/k_{off}. [c] Thermodynamic dissociation constant for the formation of the binary complex determined by dUMP titration and monitoring the accompanying fluorescence decrease. [d] Stoichiometry of dUMP binding; moles of dUMP bound per mole of dimeric enzyme. [e] Results obtained with 10 mM KPi, 50 mM 2-mercaptoethanol, 1 mM EDTA, pH 7.4, and 20 °C.

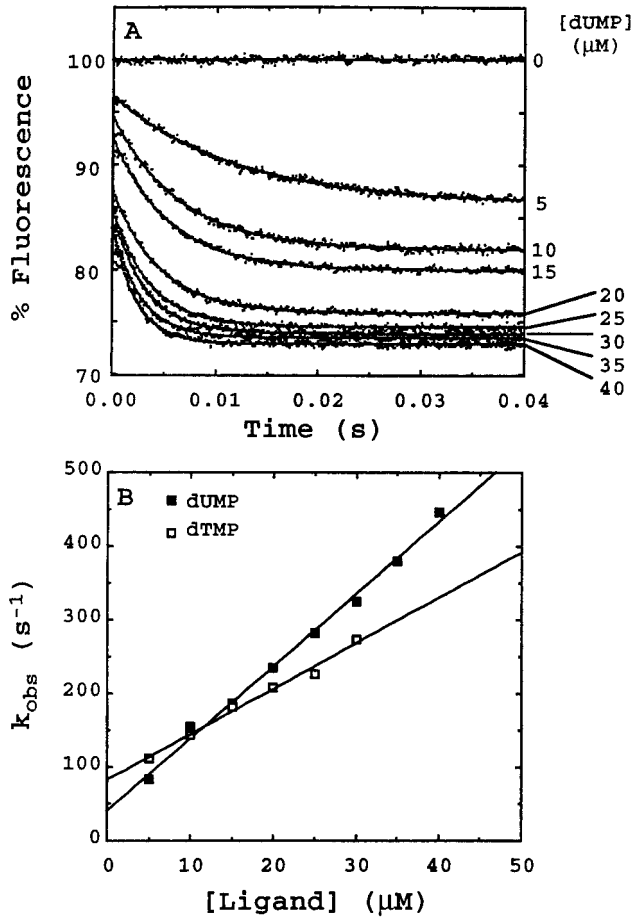

FIGURE 2: Kinetics of dUMP and dTMP binding to ecTS. (A) Time courses of fluorescence quenching as dUMP binds to ecTS. The concentration of ecTS is 1.05 μM. The enzyme was excited with light of 295 nm in order to reduce inner filter effects, and fluorescence above 320 nm was monitored. The time courses do not begin at 100% due to loss of some of the time course in the instrumental dead time and to some inner filter effects, particularly at the higher dUMP concentrations. Both experimental data points and best-fit curves are shown. The final nucleotide concentration is given within the figure. (B) Dependence of k_{obs}, the pseudo-first-order rate constant governing the time course of ligand binding to ecTS as a function of ligand concentration.

qualitatively identical to that with ecTS (unpublished results). Reconciliation of or an explanation for these striking differences in kinetics of nucleotide binding will require further experimentation.

Binding of H_2Folate to ecTS·dUMP and ecTS·dTMP. As with lcTS (Galivan et al., 1976) binding of H_2folate to ecTS could not be detected in the absence of nucleotides. When either nucleotide was present at saturating concentrations, H_2folate binding was monitored by an increase in absorbance accompanying complex formation similar to that reported for folate binding to lcTS (Lockshin et al., 1984). In accordance with the findings of other investigators, no evidence of the conversion of dTMP and H_2folate by ecTS was observed. Values of dissociation constants governing complex formation were calculated from the dependence of A_{320} on the concentration of H_2folate when enzyme with bound nucleotide was titrated with H_2folate (Table 3). Efforts to measure the kinetics of these processes by stopped-flow techniques were unsuccessful, presumably because the rate constants governing dissociation of H_2folate from these complexes are very large. For this reason, we chose to examine the kinetics of complex formation with PDDF, a tight-binding analog of H_2folate. It is likely that PDDF and H_2folate have similar association rate constants (k_{on}), but differ markedly in rates of dissociation. We found that the value of k_{on} for PDDF binding to both these complexes is large ($\sim 7 \times 10^7$ M^{-1} s^{-1}) and that k_{off} is too small to be measured by relaxation techniques, which is reported more fully below. This is consistent with the tight-binding behavior reported by others for PDDF (Pogolotti et al., 1986). If the value of k_{on} for H_2folate is similar to that measured with PDDF, then k_{off} is approximately 5000 s^{-1} (from $k_{off} = K_d/k_{on}$).[2]

Table 3: H_2Folate Binding to ecTS·dTMP and ecTS·dUMP

complex	K_d[a] (10^{-6} M)	$\Delta\epsilon_{320}$ (mM^{-1} cm^{-1})
ecTS·dUMP·H_2folate	73 ± 23	12.4 ± 1.6
ecTS·dTMP·H_2folate	66 ± 17	16.1 ± 1.6

[a] By titration. Concentrations of nucleotides and ecTS were 1 mM and 15 μM, respectively.

An additional test of the accuracy of the value of K_d for binding of H_2folate to ecTS·dTMP was performed as follows: ecTS was titrated with dTMP in the presence of 100 μM H_2folate, and apparent K_d ($K_{d,app}$) for dTMP binding was calculated. For the sequential binding of these products as shown in Scheme 1 and in the absence of catalytic reaction, $K_{d,app} = K_{dTMP}/(1 + [H_2folate]/K_{H_2folate})$, where K_{dTMP} and $K_{H_2folate}$ are K_ds for dTMP binding to ecTS and H_2folate binding to ecTS·dTMP, respectively. At 100 μM H_2folate, the measured value of $K_{d,app}$ (6.4 ± 0.6 μM) is in excellent agreement with the predicted value (5.9 μM).

Pre-Steady-State Experiments. When ecTS is mixed with both substrates to initiate catalysis, a burst of absorbance increase at 340 nm is observed (Figure 3). The burst is not unique to ecTS. We also observe a similar burst for lcTS (data not shown). This is followed by a linear increase in A_{340} with time until substrate depletion and/or product accumulation leads to a decrease in the rate. Thus the time course of increase in A_{340} can be described by an equation of the form $A_t = A° + \Delta A_{340}(1 - e^{-k_{burst}t}) + V_{ss}t$, where A_t

[2] This represents a minimum value and assumes that no other steps occur during complex formation, such as conformational changes that enhance the affinity of enzyme for H_2folate and bound nucleotide.

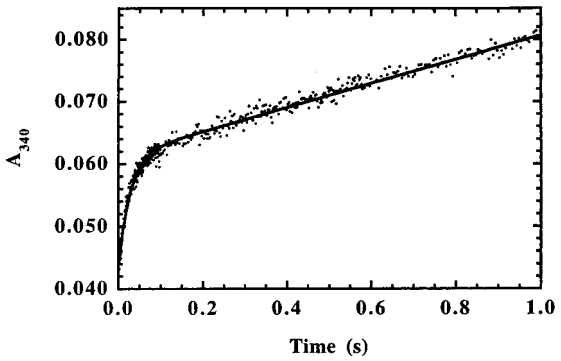

FIGURE 3: Time course of absorbance change at 340 nm when ecTS is mixed with substrates to initiate catalysis. The concentration of ecTS is 2 μM. dUMP and CH_2H_4folate are 500 and 40 μM, respectively. At this concentration of dUMP, $t_{1/2}$ for nucleotide binding is 0.13 μs so that formation of ecTS·dUMP is essentially instantaneous on the time course of this experiment. Experimental data points and best-fit curve to the equation described in the text are shown.

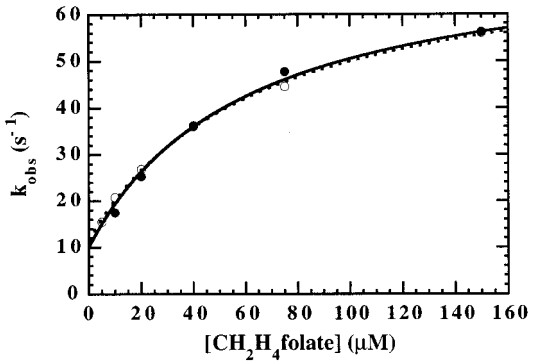

FIGURE 4: Dependence of k_{burst} on CH_2H_4folate concentration. Concentration of ecTS and dUMP are 2 and 500 μM, respectively. Values of k_{burst} were obtained by analysis of reaction time courses monitored by absorbance at 340 nm (filled circles) and by fluorescence (open circles) (excitation wavelength, 295 nm; emission wavelengths, above 350 nm). The solid line is the best-fit curve by simultaneously fitting both absorbance and fluorescence data, and the broken line is the best-fit curve to only the fluorescence data. See legend to Table 4 for additional details.

is A_{340} at time t, $A°$ is absorbance at time $t = 0$, ΔA_{340} is amplitudes of the burst phase that precede steady-state, k_{burst} is the observed first-order rate constant governing this phase, and V_{ss} is the linear rate of increase in A_{340} during steady-state. When binding of substrates is not limiting, the amplitude of the burst (ΔA_{340}) is directly proportional to the concentration of TS ($\Delta A_{340}/\mu$M ecTS $= 0.010 \pm 0.001$). One interpretation of this burst is that it represents the formation of the products H_2folate and dTMP during the first round of catalysis in which case the amount of product formed would equal 1.6 ± 0.2 μmol of products/μmol of ecTS. However, a number of lines of evidence argue against this possibility. (1) When fluorescence rather than absorbance is monitored, the burst is observed as a decrease in fluorescence intensity whereas a small linear increase in intensity accompanies product formation during steady state. (2) Such a burst of product formation is not anticipated unless dissociation of one of the products limits the overall catalytic rate, whereas for ecTS chemical transformation steps are rate determining. (3) A similar burst is observed when the inhibitor FdUMP, which forms a complex like C in Scheme 2, is used in place of dUMP. However, the linear phase corresponding to steady-state catalysis is absent in this and other non-productive complexes. (4) As with FdUMP, the amplitude of the burst is greater at 330 nm than at 340 nm, whereas the extinction maximum for the reaction is 340 nm. Furthermore, the amplitudes of the burst at 330 and 340 nm are nearly identical with dUMP and FdUMP. (5) Increases in absorbance in this wavelength range are observed in a number of complexes with TS, including those which do not catalyze reactions (for example, ecTS·dTMP·H_2folate). (6) Neither primary nor secondary isotope effects are observed on either the amplitude or rate of the burst. For these reasons we would instead propose that the increase in absorbance occurs in steps prior to the chemical reactions depicted in Scheme 2.

As shown in Figure 4, the dependence of k_{burst} on CH_2H_4-folate is hyperbolic. The simplest model consistent with such dependence is depicted in Scheme 3 where E represents ecTS·dUMP and L represents CH_2H_4folate. The initial binding of CH_2H_4folate, which can be treated as a rapid equilibrium step, is followed by a kinetically discernible reaction step preceding catalysis. For such a reaction scheme it may be shown that $k_{burst} = k_{iso}[L]/(L + K_d) + k_{r,iso} + k_{chem}$, where K_d is the dissociation constant for binding in the initial

Scheme 3: Binding Scheme for CH_2H_4folate (L) to ecTS·dUMP (E)

$$E + L \overset{K_d}{\rightleftharpoons} EL \underset{k_{r,iso}}{\overset{k_{iso}}{\rightleftharpoons}} EL^* \xrightarrow{k_{chem}} E + P$$

complex, k_{iso} and $k_{r,iso}$ are first-order rate constants governing interconversion of ecTS·dUMP·CH_2H_4folate and (ecTS·dUMP·CH_2H_4folate)*, k_{chem} is the rate constant governing the chemical conversion of substrates to products. From our analysis and assuming a k_{cat} of 1.7 s^{-1} and $k_{cat} = k_{chem}/(1 + k_{r,iso}/k_{iso})$,[3] values of K_d, k_{iso}, $k_{r,iso}$, and k_{chem} are 63 μM, 62 s^{-1}, 10 s^{-1}, and 1.8 s^{-1}, respectively. We surmise that the conversion of ecTS·dUMP·CH_2H_4folate to (ecTS·dUMP·CH_2H_4folate)* represents reorientation of a surface loop containing Arg21 and of the amino acid residues at the protein's C-terminus which serves to seal off the active site (Matthews et al., 1990a). This conformational change increases the affinity of the enzyme for the ligand 7.4-fold ($=1 + k_{iso}/k_{r,iso}$).

Kinetics of PDDF Binding. The interpretation of enzyme isomerization is consistent with results obtained with PDDF binding to wild-type and mutant ecTS. When wild-type ecTS is mixed with dUMP and PDDF, the fluorescence decreases rapidly as the ternary complex is formed (Figure 5). At high dUMP concentrations the binding of dUMP is sufficiently rapid, as indicated by the k_{on} values presented in Table 2, that the fluorescence decrease resulting from dUMP binding is not observed. The changes in fluorescence properties upon ligand binding can be utilized to determine the rate of complex formation. With respect to wild-type ecTS, the data is best described by a 2 exponential equation of the form

$$F_t = \Delta F_1 \exp^{(k_{1,obs}t)} + \Delta F_2 \exp^{(k_{2,obs}t)} + F_{equ}$$

where F_t is the fluorescence at time t, ΔF is the amplitude of the fluorescence change, k_{obs} is the rate constant for each process, and F_{equ} is the fluorescence at equilibrium. From the linear plot of k_{obs} versus the concentration of PDDF, under pseudo-first-order conditions, the association rate constant

[3] The dissociation rate constants for products are sufficiently large that they are negligible in limiting overall catalytic rate and therefore have been omitted in the definition of k_{cat}.

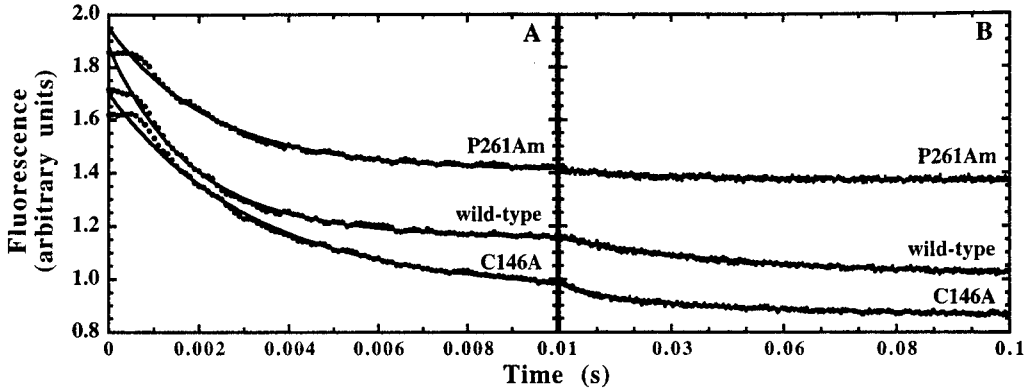

FIGURE 5: Time courses and best-fit curves of fluorescence quenching as PDDF binds to the binary complex of ecTS·dUMP, C146A·dUMP, and P261Am·dUMP. In each case, the final enzyme and dUMP concentrations are 1 μM and 500 μM, respectively. The final concentration of PDDF is 8 μM. The time courses for P261Am and C146A are offset with respect to ecTS. Panels A and B represent continued time courses over short (A) and extended (B) time ranges.

was determined to be 75 μM^{-1} s^{-1}. The slow phase is nearly independent of the concentration of PDDF (indicating that k_{off}/k_{on} must be $\ll 1$ μM) and reaches a maximum of 41 s^{-1}, which represents $k_{iso} + k_{r,iso}$. This value is similar to that observed for k_{iso} and $k_{r,iso}$ obtained from burst measurements using dUMP and CH_2H_4folate.

Evidence that this process represents reorientation of residues at the protein's C-terminus was obtained by comparing time courses observed with wild-type and mutant enzymes. Figure 5 shows representative time courses when PDDF and dUMP are mixed with wild-type ecTS, C146A, and P261Am, a mutant with the four C-terminal residues deleted. Like wild-type ecTS, the two mutants also show a fast phase and a slower phase. For both mutants the fast phase is linearly dependent on the concentration of PDDF with a k_{on} of 71 μM^{-1} s^{-1} for C146 and 58 μM^{-1} s^{-1} for P261Am. The k_{obs} for the slow phase for C146A reaches a maximum value of 36 s^{-1}. Although two exponential terms are required to define PDDF binding to P261Am, the amplitude of the second exponential is approximately 15% the amplitude observed for C146A and wild-type ecTS, indicating that this phase is not as pronounced for the truncated mutant and likely represents the conformational relocation of the C-terminus. Because of the small amplitude of this phase for P261Am an accurate determination of the maximum rate was not possible.

When PDDF binding to wild-type ecTS·nucleotide is monitored by stopped-flow absorbance spectroscopy at 340 nm, the first phase is silent. Figure 6 shows the absorbance changes accompanying PDDF binding to C146A and P261Am. The data are fitted to a single exponential equation. The maximum rate constants of 36 and 38 s^{-1} for C146A and wild-type ecTS, respectively, are in good agreement with the second process observed by fluorescence monitoring. Similar to the results obtained by fluorescence spectroscopy, the amplitude for PDDF binding to P261Am is only 10% of the amplitude observed with C146A and wild-type ecTS. The lack of the second phase for P261Am compared with C146A and wild-type enzymes indicates this process is associated with the reorientation of the C-terminus.

Because this phase is present with C146A, closure of the C-terminus does not depend on nucleophilic attack of the bound nucleotide. Our results indicate that uncoupling of conformational changes and nucleophilic attack is observed during ternary complex formation of TS, PDDF, and dUMP. Although PDDF binds rapidly and conformational changes

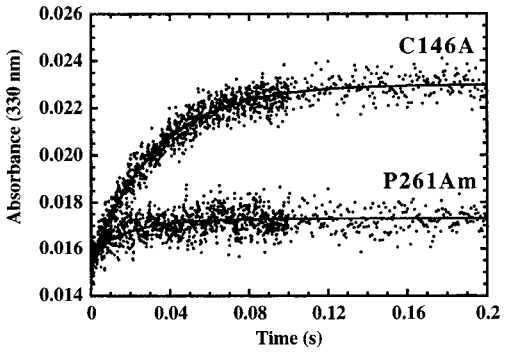

FIGURE 6: Time courses and best-fit curves for PDDF binding to the binary complexes of C146A.dUMP and P261Am.dUMP monitored by absorbance spectroscopy at 340 nm. The final concentration of enzymes and dUMP are 2 and 500 μM, respectively. The final concentration of PDDF is 8 μM. The time course for ecTS was virtually identical to that of C146A and is, therefore, not shown for clarity.

occur which are kinetically similar to those observed for CH_2H_4folate binding, Pogolottie et al. (1986) showed that formation of the covalent complex between dUMP and lcTS occurs very slowly in the presence of PDDF. Previous studies have also shown that the shift from the open form to the closed form is not required for successful attack of the bound nucleotide by the reactive site cysteine (Cisneros et al., 1993; Climie et al., 1992). These results indicate these two processes, nucleophilic attack of the bound nucleotide and conformational changes, can occur independent of one another. However, both are required to proceed past ternary complex formation and successful chemical transformation (steps 4 and 5 of Scheme 2) of bound substrates to bound products, as evidenced by the mutants P261Am and C146A.

Summary of Overall Kinetic Scheme. We have constructed an overall kinetic scheme from the kinetic and thermodynamic binding constants (Scheme 4). Key features of the scheme are as follows. Binding of substrates is ordered, with dUMP binding preceding CH_2H_4folate. The affinity of ecTS·dUMP for the latter substrate complex is weak, but is enhanced by a reaction step that probably represents C-terminus closure over the active site. Most of the chemical reactions that occur while bound substrates are converted to products are in equilibrium and are thermodynamically unfavorable. The overall reaction is driven by the reduction of an enzyme-bound exocyclic form of dTMP by bound H_4-folate. This reaction step is presumably followed by opening of the active site by movement of the C-terminus, although we do not directly observe such a step. The catalytic cycle

Scheme 4: Kinetic Scheme for Thymidylate Synthase from *E. coli*[a]

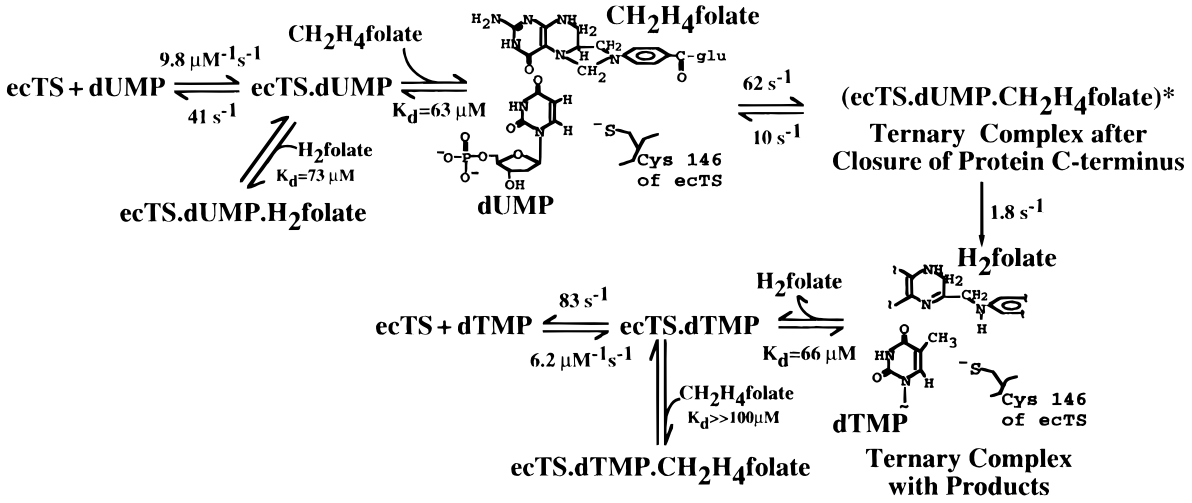

[a] The value of the rate constant governing conversion of enzyme-bound substrates to bound products was calculated from the value of k_{cat} (=1.7 s^{-1}) and from the equilibrium between ecTS·dUMP·CH_2H_4folate and (ecTS·dUMP·CH_2H_4folate)*.

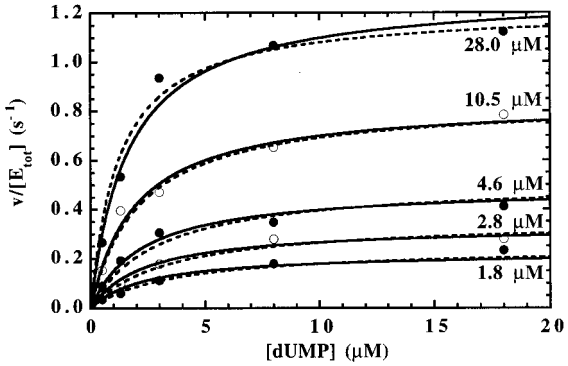

FIGURE 7: Analysis of steady-state initial velocity data to an ordered bireactant mechanism. The solid line represents the best-fit curve when the values of k_{cat}, $K_{d,dUMP}$, $K_{m,dUMP}$, and $K_{m,CH_2H_4folate}$ are unconstrained. The dashed line represents the best-fit curve when the value of k_{cat} only is unconstrained, and the remaining parameters are constrained to their experimentally determined values. Table 4 reports the parameter values obtained from these fits.

is completed by the rapid sequential dissociation of the products H_2folate and dTMP. Binding of CH_2H_4folate and H_4folate can be treated as rapid equilibrium reactions even on a stopped-flow time scale.

Steady-State Catalysis: Evaluation of Model. If the model that we have derived is correct, then it should be possible to predict the steady-state kinetics of ecTS. Values of the parameters k_{cat}, $K_{m,dUMP}$, $K_{m,CH_2H_4folate}$, and $K_{d,dUMP}$ were determined by fitting steady-state initial velocity data to the equation for an ordered bi-reactant mechanism:

$$v/E_{tot} = k_{cat}[dUMP][CH_2H_4folate]/ \{(K_{d,dUMP})(K_{m,CH_2H_4folate}) + K_{m,dUMP}[CH_2H_4folate] + K_{m,CH_2H_4folate}[dUMP] + [dUMP][CH_2H_4folate]\}$$

Experimental and fitted data are depicted in Figure 7, and best-fit parameter values are reported in Table 4. When values for steady-state kinetic constants are determined by fixing one substrate at a single high concentration while varying the other substrate (typically performed Michaelis−Menten treatment) and compared with values determined by experiments in which both substrates are varied, agreement is good. However, when values predicted from the definition of these steady-state parameters are compared with the best-fit values from the steady-state rates, agreement is poor. This is particularly true for $K_{m,dUMP}$. To address this concern, the values of the parameters $K_{d,dUMP}$ and $K_{m,CH_2H_4folate}$ were constrained to their predicted values. $K_{m,dUMP}$ was redefined as $k_{on,dUMP}/k_{cat}$ as predicted by the model, and $k_{on,dUMP}$ was constrained to its measured value of 10 μM^{-1} s^{-1}. The steady-state data was reanalyzed with k_{cat} as the only unconstrained parameter, which was found to be 1.7 s^{-1}. The resulting fit is shown as the solid line in Figure 7. Clearly the steady-state data are simulated well, and the goodness of fit is not substantially different than for the completely unconstrained fit. We conclude that values of the parameters governing steady-state rates are not accurately determined from classical analysis for this enzyme, probably due to the relative values of some of the parameters. For example, we believe that the value of 1.2 μM does not represent the true K_m for dUMP and that the value of 0.2 μM from our analysis is more accurate.

We have confirmed the order of substrate binding and product release predicted by others from product inhibition

Table 4: Comparison of Steady-State Parameter Values Obtained by Fitting Initial Velocity Data and Derived from Transient State Data

parameter	Michaelis−Menten[a]	unconstrained fit[b]	predicted by binding and transient-state data
k_{cat} (s^{-1})	1.9	1.9	1.7[c]
$K_{d,dUMP}$ (μM)	4.2	2.6	3.9[c]
$K_{m,dUMP}$ (μM)	1.2	1.2	0.2[c]
$K_{m,CH_2H_4folate}$ (μM)	11	13	10[d]

[a] Values obtained using 25 nM ecTS, 100 μM CH_2H_4folate, and varied dUMP (0−50 μM) for the determination of $K_{m,dUMP}$ and 50 μM dUMP with varied CH_2H_4folate (0−100 μM) for determination of $K_{m,CH_2H_4folate}$. Data were fit to $v/[E] = [S]k_{cat}/(K_m + [S])$. Substrate inhibition was not observed for either substrate. Values of k_{cat} are identical when either substrate was varied. [b] Steady-state data were analyzed as indicated in the text with each parameter unconstrained. [c] Steady-state data were analyzed as indicated in the text. The value of k_{cat} was unconstrained while the values of $k_{on,dUMP}$, $K_{m,dUMP}$, and $K_{m,CH_2H_4folate}$ were fixed at their predicted values. [d] The K_m for CH_2H_4folate was calculated using the thermodynamic dissociation constant for CH_2H_4folate and rate constants derived from transient state fluorescence experiments shown in Figure 4. Fitting of only fluorescence data provides a more accurate value for $k_{iso} + k_{r,iso}$ because the ligand concentration can be extended to lower concentrations. K_m was calculated using the equation: $K_{m,CH_2H_4folate} = (K_{d,CH_2H_4folate})(k_{r,iso} + k_{chem})/(k_{iso} + k_{r,iso} + k_{chem})$.

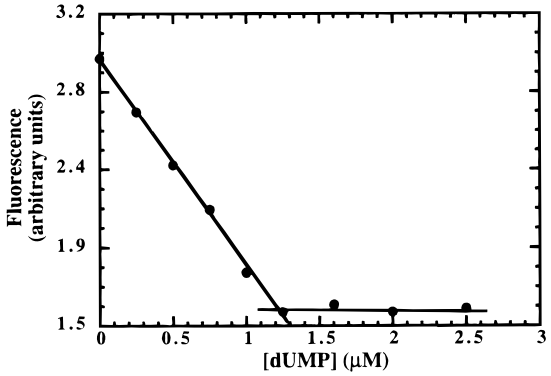

FIGURE 8: Titration of ecTS with dUMP in the presence of PDDF. The equilibrium fluorescence for 500 ms stopped-flow time courses is plotted as a function of dUMP concentration. The final concentration of PDDF is 10 μM, and that for ecTS is 1 μM (2 μM sites).

patterns for this enzyme [reviewed in Santi and Danenberg (1984)]. The products H_2folate and dTMP are only modestly potent inhibitors. No substrate inhibition is observed with dUMP and CH_2H_4folate. For dUMP, this is consistent with the predicted binding sequence. In theory, substrate inhibition might be observed with CH_2H_4folate, which is known to bind to a variety of enzyme−nucleotide complexes like ecTS·BrdUMP and ecTS·FdUMP. However, we were unable to detect CH_2H_4folate binding to ecTS.dTMP ($K_d \gg$ 100 μM) so that inhibition by this substrate was not anticipated. This poor binding is most likely due to steric hindrance between the bridge carbon of the folate and the 5-methyl group of dTMP.

Stoichiometry during Catalysis. Structural elucidation by X-ray crystallography clearly indicate that TS has two sites potentially available for catalysis and that both sites are competent to bind ligands under conditions used to produce crystals for structural studies (i.e., high protein and ligand concentrations). However, virtually every kinetic study of TS indicates that the binding sites are asymmetric with respect to ligand binding and ability to carry out catalysis. The number of sites immediately accessible (time < 0.5 s) for dUMP binding in the presence of PDDF was determined by titrating ecTS with dUMP in the presence of PDDF. As with the tight-binding TS inhbitor 1843U89 which increases the apparent affinity of TS for dUMP by 2 orders of magnitude (Weichsel et al., 1995), binding of PDDF decreases the thermodynamic dissociation constant of dUMP sufficiently to allow for an accurate measure of the number of sites immediately accessible to dUMP. We found that there are initially 1.2 dUMP binding sites per dimeric ecTS (Figure 8). Thus formation of a ternary complex with bound nucleotide and folate analog does not immediately allow access to the second site for nucleotide binding. Similarly, rapid occupancy of only one site by the covalent ternary complex ecTS−FdUMP−CH_2H_4folate is observed by spectroscopy and by isolation of the covalent complex by trichloroacetic acid precipitation (Reilly et al., 1995). The second site is occupied on a considerably slower time scale. Also, the amplitude of absorbance burst described in the preceding section is consistent with occupancy at only one site if molar extinction coefficients for complex formation are like those measured when FdUMP replaces dUMP. Our data indicate that only one of two potential catalytic sites on dimeric TS is active on the time frame of the stopped-flow measurements and transient-state catalytic experiments described in this manuscript. This view is consistent with lcTS, in which only one nucleotide binding site is observed even in the presence of folates (Galivan et al., 1976). It is not our intention to imply that occupancy of the second site is impossible, merely that availability of the site occurs relatively slowly. Furthermore, it is likely that the affinity for ligand binding at the second site is much lower than at the first. Therefore, except in the case of very tight-binding complexes or at extremely high ligand concentrations, occupancy will not be observed. Recent advances in the generation of heterodimeric enzymes will likely aid in further elucidating the mechanism of cooperativity between the two subunits which is observed with this enzyme.

Scheme 5

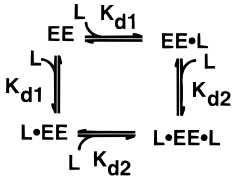

ACKNOWLEDGMENT

We thank Dr. Raymond Blakley for his many helpful discussions and suggestions during the course of this project and for his kind support. We also thank Dr. Bruce Dunlap for suggestions and comments during the drafting of the manuscript.

APPENDIX

Scheme 5 depicts the general two-site model that was utilized to evaluate ligand binding to ecTS.

General equations: L_{tot} is the total concentration of ligand L; E_{tot} is the total concentration of enzyme; EE·L and L·EE are equivalent species, thus

$$E_{tot} = [EE] + [EE{\cdot}L] + [L{\cdot}EE{\cdot}L]$$

[L] is determined by solving for the root of

$$L^3 + (K_{d2} + 2E_{tot} - L_{tot})L^2 + (K_{d1}/2 + E_{tot} - L_{tot})K_{d2}L - (K_{d1}/2)K_{d2}L_{tot}$$

where $0 \le [L] \le L_{tot}$. The concentration of enzyme forms are calculated from

$$[EE] = E_{tot}/\{1 + 2L/K_{d1}(1 + L/K_{d2})\}$$

$$[EE{\cdot}L] = 2[EE][L]/K_{d1}$$

$$[L{\cdot}EE{\cdot}L] = [EE{\cdot}L][L]/K_{d2}$$

Fluorescence F is calculated from

$$F = f_E[EE] + f_{EL}(EE{\cdot}L) + f_{EL2}[L{\cdot}EE{\cdot}L] \qquad (1)$$

where f's are coefficients representing fluorescence/unit concentration for each species.

Best-fit values of parameters E_{tot}, K_{d1}, K_{d2}, f_E, f_{EL}, and f_{EL2} can be calculated from the dependence of fluorescence on L_{tot}.

When $E_{tot} \ll K_d$s,

$$F = (F_E + 2F_{EL}[L_{tot}]/K_{d1} + 2F_{EL2}[L_{tot}]^2/K_{d1}K_{d2})/(1 + 2[L_{tot}]/K_{d1} + 2[L_{tot}]^2/K_{d1}K_{d2}) \qquad (2)$$

where the *F*'s are fluorescence intensities contributed by the different enzyme complexes.

Consider the case when L represents a nucleotide like dUMP. At a low enzyme concentration like that in Figure 1B there is no evidence for the existence of L·EE·L from the dependence of *F* on $[L_{tot}]$ when analyzed with eq 2; that is, all terms containing $[L_{tot}]^2$ can be omitted (yielding a single-site model) without altering the quality of fit or the calculated value of K_{d1} in any way. At a high enzyme concentration like that in Figure 1C, there is still no evidence for the existence of L·EE·L. Fitted values of K_{d2} are high compared to the experimental range of ligand concentration employed. Furthermore, the fitted value for f_{EL2} is nearly identical to that for f_{EL}, which would indicate that binding to the second site was spectrally silent (an unlikely proposition). The solid line in Figure 1C represents the best-fit curve obtained when K_{d2} is infinitely large (i.e., a single-site model), and the dashed line represents the best fit in a limiting case where $K_{d1} = K_{d2}$ and $f_E - f_{EL} = f_{EL} - f_{EL2}$; that is, the binding sites do not interact and fluorescence decrease upon binding at one site is independent of the state of ligation of the other site. In conclusion, the experimental data for nucleotide binding is entirely consistent with single site occupancy but cannot exclude the possibility of binding to the second site at very high ligand concentrations.

To allow for symmetry in the binding model, K_d values reported in Table 2 are equal to $K_{d1}/2$ in the above analysis. Thus K_d is the macroscopic binding constant (K_d = [ecTS]-[L]/[ecTS·L], where the concentration of ecTS is the concentration of dimeric enzyme rather than the subunit concentration) for nucleotide binding.

REFERENCES

Appleman, J. R., Howell, E. E., Kraut, J., Kuhl, M., & Blakley, R. L. (1988a) *J. Biol. Chem. 263*, 9187−9198.

Appleman, J. R., Prendergast, N., Delcamp, T. J., Freisheim, J. H., & Blakley, R. L. (1988b) *J. Biol. Chem. 263*, 10304−10313.

Appleman, J. R., Spencer, H. T., & Villafranca, J. E. (1991) *Pteridines 3*, 127−129.

Aull, J. L., Lyon, J. A., & Dunlap, R. L. (1974). *Arch. Biochem. Biophys. 165*, 805−808.

Beard, W. A., Appleman, J. R., Huang, S., Delcamp, T. J., Freisheim, J. H., & Blakley, R. L. (1991) *Biochemistry 30*, 1432−1440.

Bradshaw, T. P., & Dunlap, R. B. (1993) *Biochim. Biophys. Acta 1163*, 165−175.

Carreras, C. W., & Santi, D. V. (1995) *Annu. Rev. Biochem. 64*, 721−762.

Carreras, C. W., Climie, S. C., & Santi, D. V. (1992) *Biochemistry 31*, 6038−6044.

Cisneros, R. J., Zapf, J. W., & Dunlap, R. B. (1993) *J. Biol. Chem. 268*, 10102−10108.

Climie, S., & Santi, D. V. (1990) *Proc. Natl. Acad. Sci. U.S.A. 87*, 633−637.

Climie, S. C., Carreras, C. W., & Santi, D. V. (1992) *Biochemistry 31*, 6032−6038.

Davisson, V. J., Sirawaraporn, W., & Santi, D. V. (1989) *J. Biol. Chem. 264*, 9145−9148.

Dev, I. K., Yates, B. B., Leong, J., & Dallas, W. S. (1988) *Proc. Natl. Acad. Sci. U.S.A. 85*, 1472−1476.

Dev, I. K., Dallas, W. S., Ferone, R., Hanlon, M., Mckee, D. D., & Yates, B. B. (1994) *J. Biol. Chem. 269*, 1873−1882.

Edman, U., Edman, J. C., lundgren, B., & Santi, D. V. (1989) *Proc. Natl. Acad. Sci. U.S.A. 86*, 6503−6507.

Finer-Moore, J. S., Fauman, E. B., Foster, P. C., Perry, K. M., & Santi, D. V., Stourd, R. M. (1993) *J. Mol. Biol. 232*, 1101−1116.

Finer-Moore, J. S., Maley, G., Maley, F., & Stroud, RM. (1994) *Biochemistry 33*, 15459−15468.

Galivan, J., Maley, F., & Baugh, C. M. (1977) *Arch. Biochem. Biophys. 184*, 346−354.

Galivan, J. H., Maley, F., & Baugh, C. M. (1976) *Biochem. Biophys. Res. Commun. 71*, 527−534.

Hardy, L. W., Finer-Moore, J. S., Montfor, W. R., Jones, M. O., Santi, D. V., & Stroud, R. M. (1987) *Science 235*, 448−455.

Hardy, L. W., Graves, K. L., & Nalivaika, E. (1995) *Biochemistry 34*, 8422−8432, 1995.

Kamb, A., Finer-Moore, J. S., & Stroud, R. M.,(1992) *Biochemistry 31*, 12876−12884.

Kunkel, T. A. (1985) *Proc. Natl. Acad. Sci. U.S.A. 82*, 488−492.

LaPat-Polasko, L., Maley, G., & Maley, F. (1990) *Biochemistry 29*, 9561−9572.

Lockshin, A., Mondal, K., & Danenberg, P. V. (1984) *J. Biol. Chem. 259*, 11346−11352.

Maley, G. F., & Maley F. (1988) *J. Biol. Chem. 263*, 7620−7627.

Matthews, D. A., Appelt, K., Oatley, S. J., & Xuong, N. H. (1990a) *J. Mol. Biol. 214*, 923−936.

Matthews, D. A., Villafranca, J. E., Janson, C. A., Smith, W. W., Welsh, K., & Freer, S. (1990b) *J. Mol. Biol. 214*, 937−948.

Michaels, M. L., Kim, C. W., Matthews, D. A., & Miller, J. H. (1990) *Proc. Natl. Acad. Sci. U.S.A. 87*, 3957−3961.

Mittelstaedt, D. M., & Schimerlic, M. (1986) *Arch. Biochem. Biophys. 245*, 417−425.

Montfort, W. R., Perry, K. M., Fauman, E. B., Finner-Moore, J. S., Maley, G. F., Hardy, L., Maley, F., & Stroud, R. M. (1990) *Biochemistry 29*, 6964−6977.

Moore, M. A., Ahmed, F., & Dunlap, R. B. (1986a) *J. Biol. Chem. 261*, 12745−12749.

Moore, M. A., Ahmed, F., & Dunlap, R. B. (1986b) *Biochemistry 25*, 3311−3317.

Perry, K. M., Fauman, E. B., Finer-Moore, J. S., Montfort, W. R., Maley, G. F., Maley, F., & Stroud, R. M. (1990) *Proteins: Struct., Funct., Genet. 8*, 315−333.

Pinter, K., Davisson, V. J., & Santi, D. V. (1988) *DNA 7*, 235−241.

Pogolotti, A. L., Danenberg, P. V., & Santi, D. V. (1986) *J. Med. Chem. 29*, 478−482.

Reilly, T. R., Barbour, K. W., Dunlap, R. B., & Berger, F. G. (1995) *Mol. Pharmacol. 48*, 72−79.

Santi, D. V., & Danenberg, P. V. (1984) in *Folates and Pterins, Vol. 1: Chemistry and Biochemistry of Folates* (Blakley, R. L., & Benkovic, S. J. Eds.) pp 345−398, Wiley-Interscience, New York.

Santi, D. V., McHenry, C. S., & Sommer, H. (1974) *Biochemistry 13*, 471−481.

Shiffer, C. A., Clifton, I. J., Davisson, V. J., Santi, D. V., & Stoud, R. M. (1995) *Biochemistry 34*, 16279−16287.

Singer, S. C., Richards, C. A., Ferone, R., Benedict, D., & Ray, P. (1989) *J. Bacteriol. 171*, 1372−1378.

Villafranca, J. E., Howell, E. E., Voet, D. H., Stobel, M. S., Ogden, R. C., Abelson, J. N., & Kraut, J. (1983) *Science 222*, 782−788.

Weichsel, A., Montfort, W., Ciesla, J., & Maley, F. (1995) *Proc. Natl. Acad. Sci. U.S.A. 92*, 3493−3497.

Zhang, H., Cisneros, R. J., Dunlap, R. B., & Johnson, L. F. (1989) *Gene 84*, 487−491.

Zhang, H., Cisneros, R. J., Deng, W., Johnson, L. F., & Dunlap, R. B. (1990) *Biochem. Biophys. Res. Commun. 167*, 869−875.

BI961794Q